A High-Efficiency Dimmable LED Driver for Low-Power Lighting Applications

Huang-Jen Chiu, *Senior Member, IEEE*, Yu-Kang Lo, *Member, IEEE*, Jun-Ting Chen, Shih-Jen Cheng, Chung-Yi Lin, and Shann-Chyi Mou

Abstract—This paper presents a dimmable light-emitting diode (LED) driver with adaptive feedback control for low-power lighting applications. An improved pulsewidth modulation dimming technique is studied for regulating the LED current and brightness. Under universal input voltage operation, high efficiency and high power factor can be achieved by a coupled inductor single-ended primary inductance converter power factor correction (PFC) converter with a simple commercial transition-mode PFC controller. The operation principles and design considerations of the studied LED driver are analyzed and discussed. A laboratory prototype is also designed and tested to verify the feasibility.

Index Terms—Coupled inductor single-ended primary inductance converter power factor correction (SEPIC PFC), dimmable light-emitting diode (LED) driver, universal input voltage.

I. INTRODUCTION

LIGHT-EMITTING diode (LED) gradually becomes a commonly used solid-state light source in general lighting applications. It has longer lifetime and has no poison mercury content compared with the conventional fluorescent lamp [1]–[5]. Multiple LED lamps are usually connected in parallel for obtaining enough lighting levels. In addition, dimming control is often needed to regulate lighting levels for human needs as well as to achieve energy saving. A conventional linear current-regulator method, as shown in Fig. 1(a), has simple circuit configuration. It is widely used for dimming applications by modulating the current amplitude of the parallel-connected LED lamps [6]. However, linear dimming is not recommended at currents lower than the test conditions because it may produce unpredictable results and may be subjected to variation in performance. As shown in Fig. 1(b), a pulsewidth modulation (PWM) dimming method can be used to dim the LED lamp by modulating its pulse current width. The corresponding PWM controller series connected with every LED lamp raises the circuit complexity and cost. Furthermore, the uncontrollable current amplitude will shorten the lifetime of the LED lamp

[7], [8]. A novel LED driver with self-adaptive drive voltage was presented in [9]. The authors realized an adaptive voltage adjustment by sensing the gate-source voltage V_{GS} of the dimming transistors. The studied LED driver is a current-mode controlled single-ended primary inductance converter (SEPIC) with 20–30-V dc input voltage. A sequential phase-shifted PWM dimming scheme is also used to adjust LED string brightness individually for reducing the input/output current ripple. Every LED string has an individual PWM controller. In general lighting applications, ac input current harmonics have to also meet IEC 61000-3-2 Class C regulations for output power over 25 W [10]–[16]. A transition-mode (TM) SEPIC power factor correction (PFC) circuit shown in Fig. 2(a) is commonly used to achieve high power factor and low harmonics for low-power lighting applications with single-voltage input (115 V_{AC}/230 V_{AC}). A large input filter is necessary for eliminating high current ripple on the TM input current. Extra power loss on the input filter is undesirable. As shown in Fig. 2(b), the SEPIC PFC converter can be operated in continuous current conduction mode (CCM) to reduce the input current ripple under universal voltage input operation (90−270 V_{AC}). A complicated control circuit, e.g., average current controller, is generally necessary. Thus, it is unsuitable for low-power lighting applications [17]–[21]. In this paper, a coupled inductor SEPIC PFC converter is studied for driving multiple LED lamps. The CCM operation on input current can be achieved by using a commercial low-cost TM PFC control IC. An improved PWM dimming technique is also studied and implemented for regulating simultaneously the amplitude and pulsewidth of the LED current.

II. OPERATION PRINCIPLE AND STEADY-STATE ANALYSIS

As shown in Fig. 3, the studied LED driver consists of a coupled inductor SEPIC PFC converter, an improved PWM dimming circuit, and an adaptive feedback controller. The input current can be operated at CCM condition by using a commercial low-cost TM PFC control IC. High power factor can be achieved without an additional input filter for eliminating high-frequency current ripple. The output voltage of the coupled inductor SEPIC PFC converter can be adjusted by the studied adaptive feedback controller to minimize the power losses on the dimming transistors. Compared with the conventional PWM dimming scheme that the pulsewidth of every LED lamp current is modulated by the individual PWM controller, the studied dimming circuit uses only one simple PWM controller to modulate all of the LED lamps' pulsewidth.

H.-J. Chiu, Y.-K. Lo, J.-T. Chen, S.-J. Cheng, and C.-Y. Lin are with the Department of Electronic Engineering, National Taiwan University of Science and Technology, Taipei 10607, Taiwan (e-mail: hjchiu@mail.ntust.edu.tw; yklo@mail.ntust.edu.tw; D9302406@mail.ntust.edu.tw; aln0629@yahoo.com.tw; B9102032@mail.ntust.edu.tw).

S.-C. Mou is with the Department of Mechanical Engineering, Ching-Yun University, Jung-Li 320, Taiwan (e-mail: msc@cyu.edu.tw).
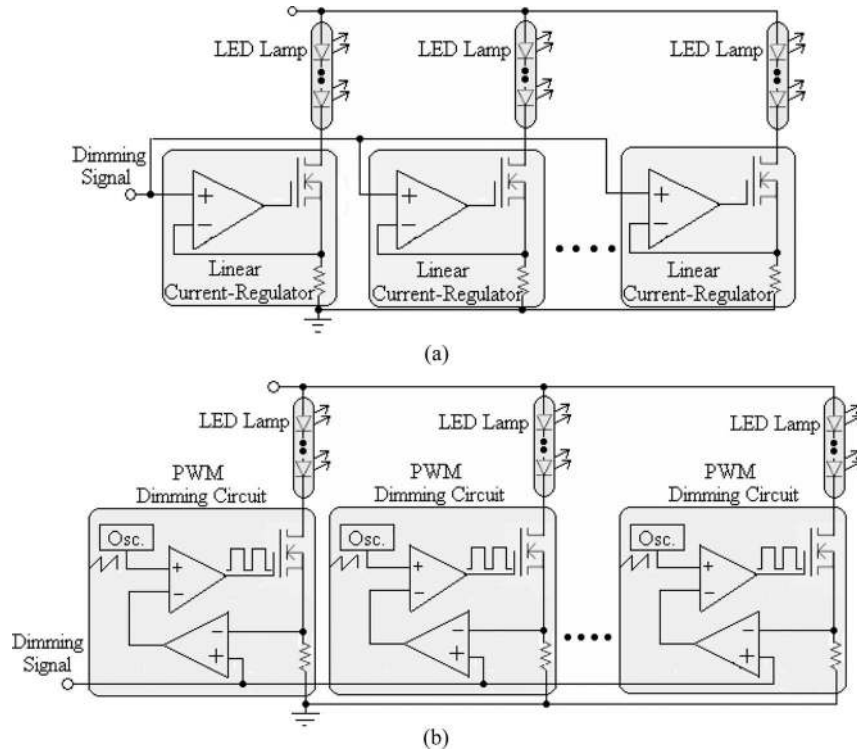
Fig. 1.   Conventional (a) linear current regulator and (b) PWM dimming methods.
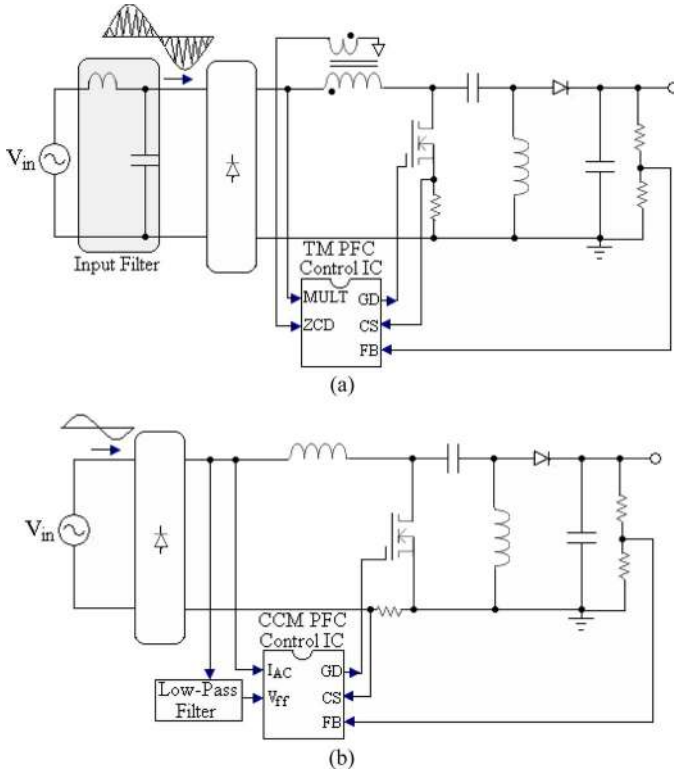

Fig. 2.   (a) TM SEPIC PFC converter and (b) CCM SEPIC PFC converter.

Fig. 4(a) shows the theoretical waveforms of the studied LED dimming circuit. The current pulsewidth T_{on} and average brightness of the parallel-connected LED lamps can be modulated by a simple low-frequency PWM controller. During on-time interval of the PWM dimming, the amplitude of LED lamp current is regulated by a linear current regulator to be oper-

ated at a specific condition suggested by the LED's datasheet. Fig. 4(b) shows the small-signal equivalent circuit of the linear current regulator. The transfer function T_d can be derived as

$$T_d = \frac{I_{\text{LED}}}{V_m} = \frac{g_m A_v / (1 + g_m R_d)}{1 + R_d g_m A_v / (1 + g_m R_d)} \approx \frac{1}{R_d} \quad (1)$$

where g_m is the transconductance gain of the dimming MOSFET Q_d, A_v is the open-loop voltage gain of the operational amplifier, and R_d denotes the dimming resistor. Based on (1), the amplitude I_p of the LED current in Fig. 4(a) can be regulated by the modulating voltage V_m as

$$I_{\text{LED}} = \frac{V_m}{R_d}. \quad (2)$$

Assuming that the turn ratio (N_s/N_p) of the coupled inductor is larger than one, the theoretical waveforms of the coupled inductor SEPIC PFC converter are shown in Fig. 5. There are three switching modes within an operating cycle. Referring to the equivalent circuits in Fig. 6, the operation principle of the studied coupled inductor SEPIC PFC converter can be explained in detail.

1) Mode 1 $(t_0 - t_1)$: At t_0, power switch Q is on, and output diode D_o is off. During this time interval, the current $I_{L_{lk1}}$ increases linearly, and the leakage inductor L_{lk1} stores energy. Since the turn ratio of the coupled inductor is larger than one, the current $|I_{in}|$ deceases linearly, and the leakage inductor L_{lk2} releases energy.

2) Mode 2 $(t_1 - t_2)$: At t_1, power switch Q is off. The output diode D_o handles the currents $|I_{in}|$ and $I_{L_{lk1}}$. During this time interval, the current $I_{L_{lk1}}$ decreases linearly, and the current $|I_{in}|$ increases linearly.
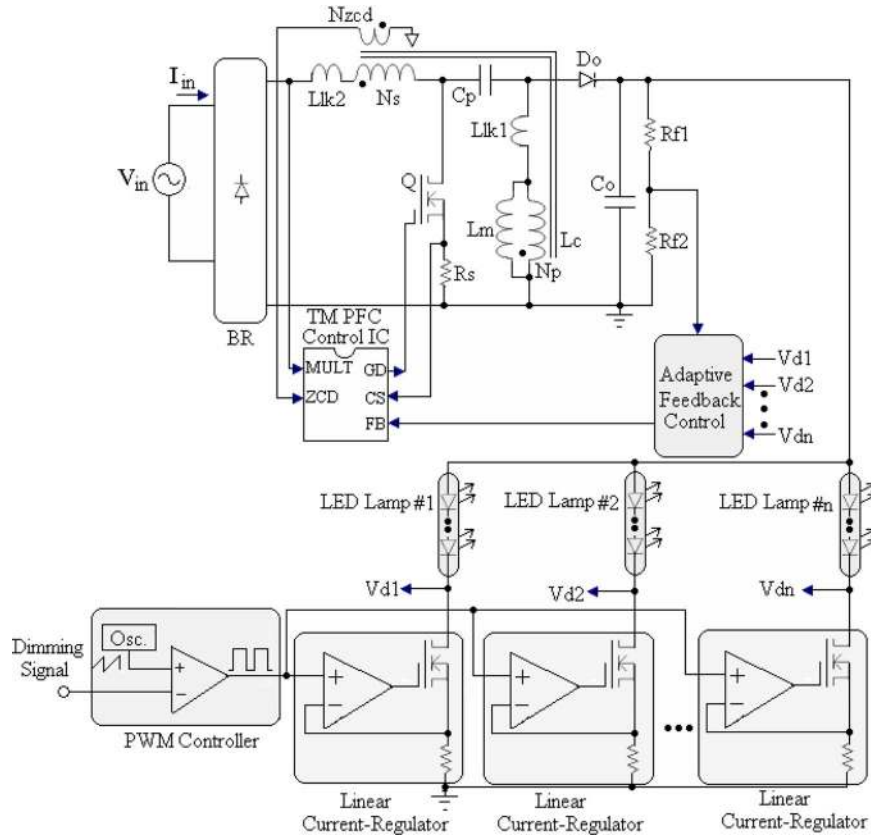
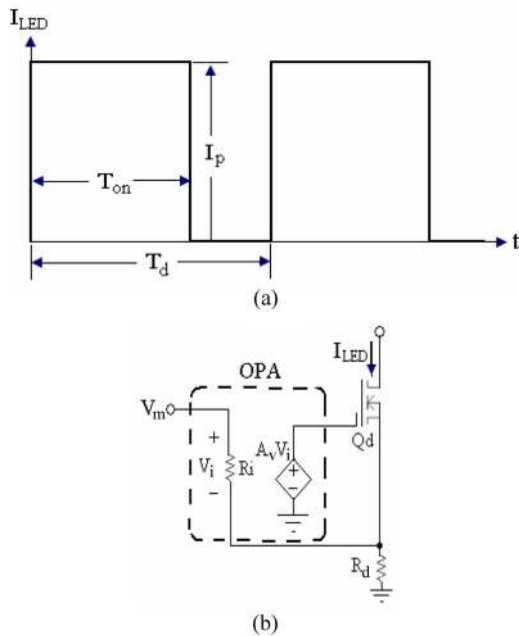Fig. 3. Studied LED driver with an improved PWM dimming circuit.

Fig. 4. (a) Theoretical dimming waveforms and (b) equivalent circuit of linear current regulator.

Fig. 5. Theoretical waveforms of the coupled inductor SEPIC PFC converter.

3) Mode 3 $(t_2 - t_3)$: At t_2, the current $I_{L_{1k}1}$ reaches to zero and changes its direction. During this time interval, the current $I_{L_{1k}1}$ remains decreasing, and the current $|I_{in}|$ remains increasing. At t_3, the summation of the currents $|I_{in}|$ and $I_{L_{1k}1}$ reaches to zero, and the power switch Q is then turned on. The output diode D_o is turned off under
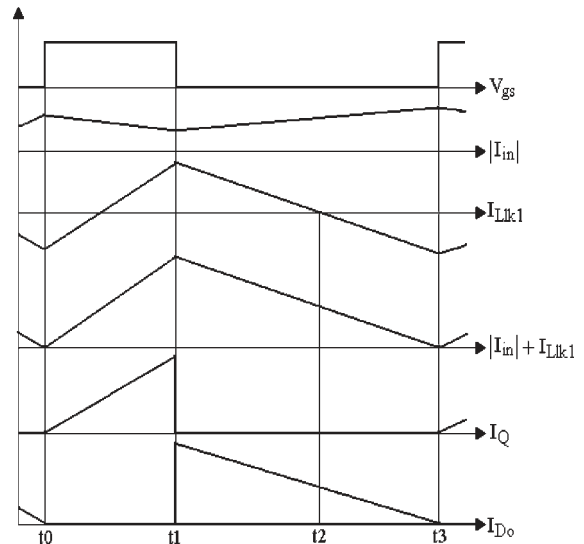
zero-current condition without reverse-recovery loss. The circuit operation then returns to Mode 1.

According to the voltage–second balance relationship for the two equivalent inductances L_{e1} and L_{e2} of the coupled inductor, the output voltage V_o and the coupling capacitor voltage V_b can be derived as

$$V_o = \frac{\delta}{1-\delta}|V_{in}| \tag{3}$$
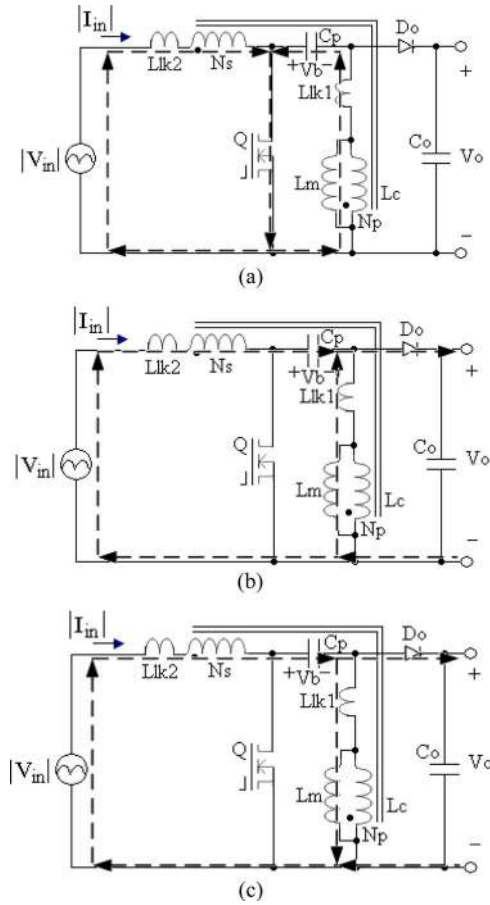
$$V_b = |V_{in}| \tag{4}$$

Fig. 6. Equivalent circuits under different switching modes.

where δ represents the duty cycle of the power switch Q. Thus, the voltage across both sides of the coupled inductor is $|V_{in}|$ as Q is on, while the voltage across both sides of the coupled inductor is V_o as Q is off.

III. DESIGN CONSIDERATIONS

The design considerations for the key components of the studied dimmable LED driver will be discussed in detail as follows.

A. Dimming Circuit Design

Fig. 7 shows a schematic diagram of the studied dimming circuit. The PWM dimming signal is generated by a commercial low-cost PWM control IC (TL494) and is then voltage-divided by the resistors R_3 and R_4 to a specific modulating voltage V_m. The current pulsewidth of the parallel-connected LED lamps can be adjusted by the PWM dimming signal. The dimming frequency is usually higher than 70 Hz, making them perceivable to the human eye. Considering the switching loss for the dimming transistors, the dimming frequency in this paper is designed at 400 Hz. During on-time interval of the PWM dimming, the amplitude of LED lamp current is regulated by a linear current regulator to be operated at a specific condition suggested by the LED's datasheet. The linear current regulator consists of an operational amplifier LM358, a
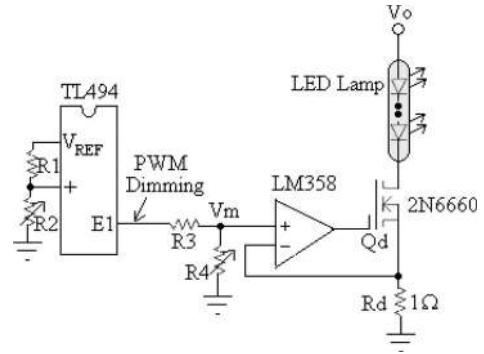

Fig. 7. Schematic diagram of the dimming circuit.

dimming transistor 2N6660, and a dimming resistor R_d. In this paper, the used LED lamp is composed of 13 pieces of series-connected LUMILEDS emitter-type LEDs. This LUMILEDS diode is a 1.2-W high-luminance LED with a nominal voltage of 3.42 V at a rated current of 350 mA. For a given dimming resistor R_d of 1 Ω, the modulating voltage V_m during on-time interval can be determined based on (2) as follows:

$$V_m = I_{LED} \times R_d = 0.35 \text{ V}.$$

The power rating of the dimming resistor R_d can then be calculated as follows:

$$P_{R_d} = I_{LED}^2 \times R_d = 122.5 \text{ mW}.$$

As shown in Fig. 7, any LED failure will result in extinguishment of the corresponding LED lamp. This problem can be solved by a bypass design for LED failure [6]. Every LED is parallel connected with a Zener diode. Under normal operation, the voltage across the LED does not reach the breakdown voltage of the Zener diode, and the current flows through the LED. When a LED fails, the LED current can flow through the parallel-connected Zener diode, and the LED lamp will not extinguish. The reliability of the LED lighting system can be improved by the bypass design.

B. Coupled Inductor Design

Assuming that the voltages applied to the primary and secondary sides of the coupled inductor are V_p and V_s, respectively, the relationship equations of the magnetizing current I_m, the leakage inductance current I_{lk1} of the coupled inductor, and the rectified input current $|I_{in}|$ can then be derived as follows:

$$V_p = L_{lk1} \times \frac{dI_{lk1}}{dt} + L_m \times \frac{dI_m}{dt} \tag{5}$$

$$V_s = L_{lk2} \times \frac{d|I_{in}|}{dt} + \frac{N_s}{N_p} \times L_m \times \frac{dI_m}{dt} \tag{6}$$

$$\frac{dI_m}{dt} = \frac{dI_{lk1}}{dt} + \frac{N_s}{N_p} \times \frac{d|I_{in}|}{dt} \tag{7}$$

where L_{lk1} and L_{lk2} represented the primary and secondary leakage inductances of the coupled inductor and L_m denotes the magnetizing inductance. Taking into consideration the application of the same voltage toward both sides of the coupled
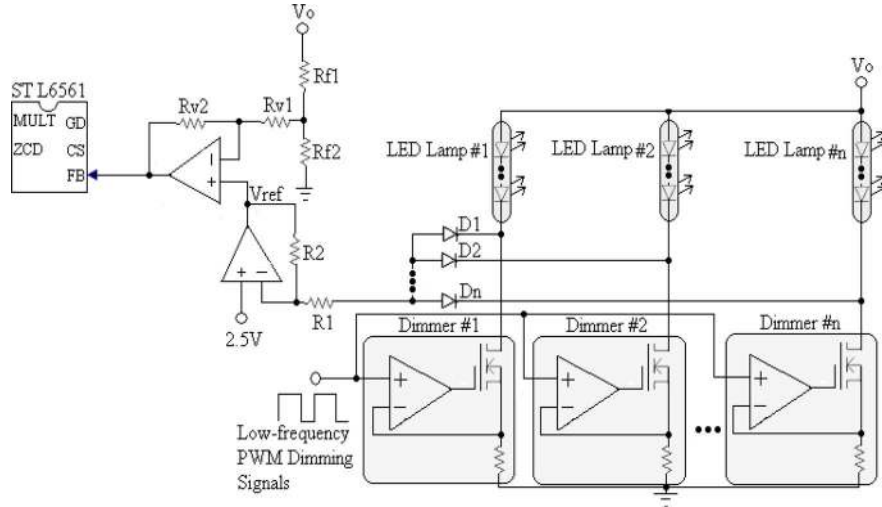
Fig. 8.   Adaptive feedback control circuit.

inductor, the winding voltages V_p and V_s can be represented as follows:

$$V_p = L_{e1} \times \frac{dI_{lk1}}{dt} \tag{8}$$

$$V_s = L_{e2} \times \frac{d|I_{in}|}{dt} \tag{9}$$

$$L_{e1} = \frac{L_{lk1} \times L_{lk2} + L_m \times L_{lk2} + (N_s/N_p)^2 \times L_m \times L_{lk1}}{L_{lk1} + N_s/N_p \times (N_s/N_p - 1) \times L_m} \tag{10}$$

$$L_{e2} = \frac{L_{lk1} \times L_{lk2} + L_m \times L_{lk2} + (N_s/N_p)^2 \times L_m \times L_{lk1}}{L_{lk1} - (N_s/N_p - 1) \times L_m}. \tag{11}$$

Supposing that the leakage inductance L_{lk2} is neglected in secondary side, then the following relationship equation can be given:

$$\frac{V_s}{V_p} = \frac{N_s}{N_p} \frac{L_m}{L_m + L_{lk1}}. \tag{12}$$

Because the same voltage is applied to both sides of the coupled inductor, the equivalent inductances L_{e1} and L_{e2} can be simplified as follows:

$$L_{e1} = L_m + L_{lk1} \tag{13}$$

$$L_{e2} = \infty. \tag{14}$$

Thus, the input equivalent inductance will be indefinitely large and will result in free-ripple input current as long as the following relationship equation is satisfied:

$$n = \frac{N_s}{N_p} = 1 + \frac{L_{lk1}}{L_m}. \tag{15}$$

In this paper, a simple TM PFC control IC (ST L6561) is used for achieving high power factor input and output voltage regulation of the LED driver. As mentioned earlier, a ripple-free input current can be assured as long as (15) is satisfied. By using the design equations in application note of L6561,

the equivalent inductance L_e of the coupled inductor can be determined as follows [22], [23]:

$$L_e = L_{e1} // L_{e2} = \frac{f(k_{v,min})}{1 + k_{v,min}} \frac{V_{in,min}^2}{f_{s,min}P_{in,max}} \tag{16}$$

$$f(k_{v,min}) = \frac{1}{T_l} \int_0^{T_l} \left[\frac{\sin^2(2\pi f_l t)}{1 + k_{v,min} |\sin(2\pi f_l t)|} \right] dt \tag{17}$$

$$k_{v,min} = \frac{\sqrt{2}V_{in,min}}{V_o} \tag{18}$$

where T_l is the line period, $P_{in,max}$ is the maximum input power, and $V_{in,min}$ is the minimum input voltage. The magnetizing inductance L_m, leakage inductance L_{lk1}, and turn ratio n of the coupled inductor can be determined based on (13)–(16).

C. Coupling Capacitor Design

For the theoretical waveform analysis in Section II, the capacitor voltage V_b is considered constant in one switching cycle and follows the source voltage in a line period. Anyway, there is a voltage ripple due to the input inductor current flowing through capacitor C_p. For a given maximum voltage ripple $\triangle V_b$, the coupling capacitor C_p can be selected as follows:

$$C_p = \frac{L_e}{\Delta V_b} \frac{I_{in,max}^2}{(V_o + \sqrt{2}V_{in,min})}. \tag{19}$$

D. Adaptive Feedback Control Design

As mentioned earlier, a simple TM PFC control IC (ST L6561) is used for achieving high power factor input and output voltage regulation of the LED driver. The bandgap and the forward voltage of the LED may decrease in accordance with increasing operation time because the junction temperature changes with power dissipation and ambient temperature as well as device aging. A constant output voltage design for the LED driver circuit will cause serious power dissipations on dimming circuit under dimming operation [24]–[26]. Thus, an adaptive feedback control, as shown in Fig. 8, is designed
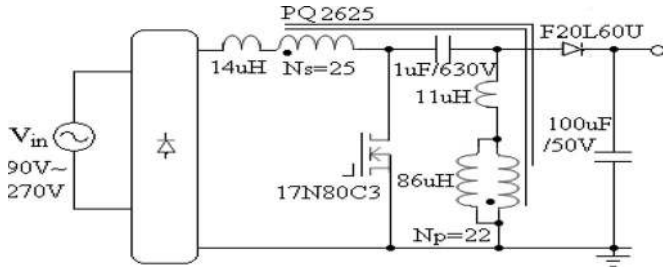
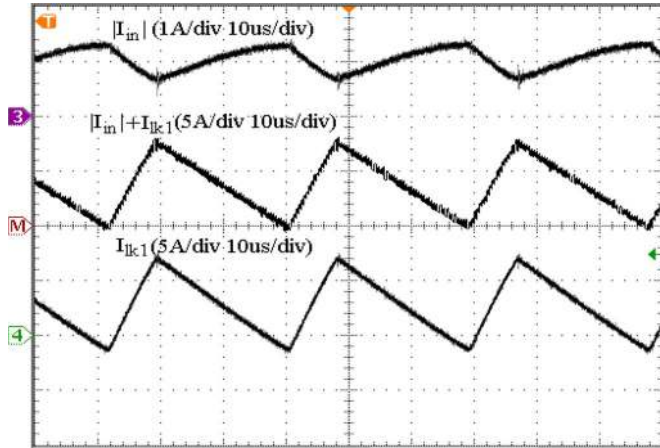Fig. 9.   Schematic diagram of the laboratory prototype.
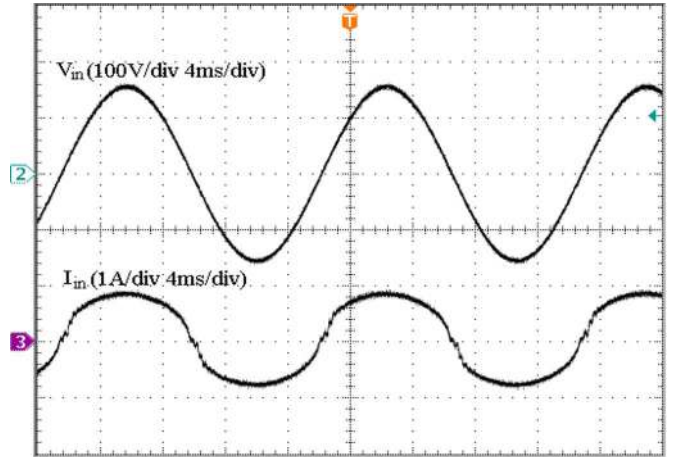

Fig. 10.   Measured inductor current waveforms.

to minimize the power losses on the dimming transistors. The drain voltage of the dimming transistors is sensed to determine the proper reference voltage V_{ref} in the voltage feedback control loop. The output voltage of the LED driver can be adjusted so that the dimming transistors are operated with a minimum voltage drop.

IV. EXPERIMENTAL VERIFICATIONS

To verify the feasibility of the studied dimmable LED driver, a laboratory prototype with the following specifications was designed and tested:

1) input voltage: 90–270 V;
2) rated output power: 60 W;
3) rated output current: 1.4 A.

Fig. 9 shows a schematic diagram of the laboratory prototype. Based on (13)–(16), the design parameters L_m, L_{lk1}, and n of the coupled inductor can be selected as 86 μH, 11 μH, and 1.13. A 14 μH of the secondary leakage inductance L_{lk2} was measured. From (19), the coupling capacitor C_p can be selected as 1 μF for giving a 15 V of maximum dc bus voltage ripple. The measured inductor current waveforms of the prototype circuit are shown in Fig. 10. It can be observed that a CCM input current is obtained while the summation current of the rectified input current $|I_{\text{in}}|$ and the current I_{lk1} is operated under TM. It is agreed with the theoretical analysis shown in Fig. 5. The large input filter in a conventional TM PFC circuit is not needed for the studied coupled inductor SEPIC PFC circuit using a TM PFC control IC. The measured input voltage V_{in} and current I_{in} at the input voltages of 110 and 220 V are shown in

(a)
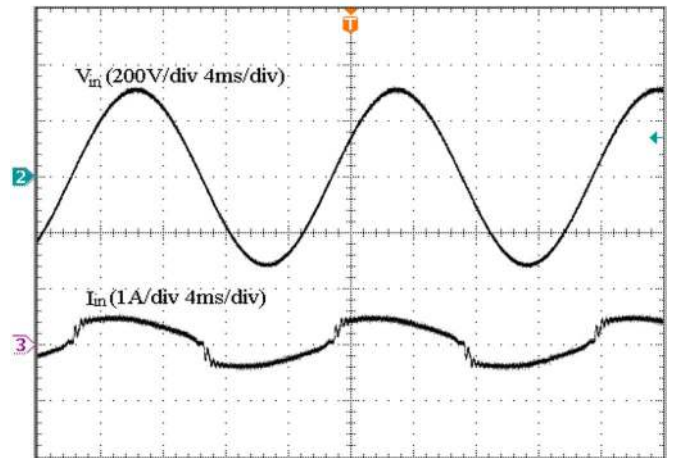
(b)

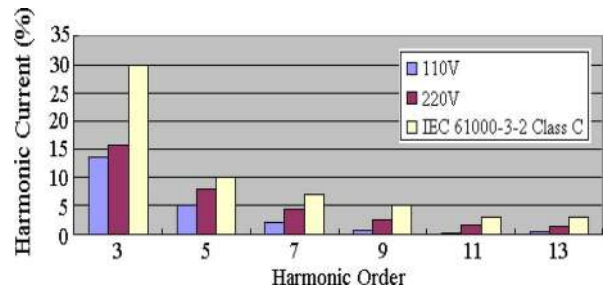Fig. 11.   Measured input current waveforms at (a) 110 V and (b) 220 V.

Fig. 12.   Measured input current harmonics.

Fig. 11(a) and (b), respectively. The input current I_{in} has a near-sinusoidal waveform and is in phase with the input voltage V_{in}.

Fig. 12 shows the measured input current harmonics at the input voltages of 110 and 220 V. It is obvious that the current harmonics are satisfied with the IEC 61000-3-2 class C regulation. Efficiency and power factor variations under different input voltage are shown in Fig. 13. Under universal input voltage operation, conversion efficiency over 0.93 and power factor over 0.91 can be achieved. Meanwhile, Fig. 14 shows the output diode current waveform. The reverse-recovery loss on the output diode D_o can be eliminated due to its zero-current-switching turn-off feature.
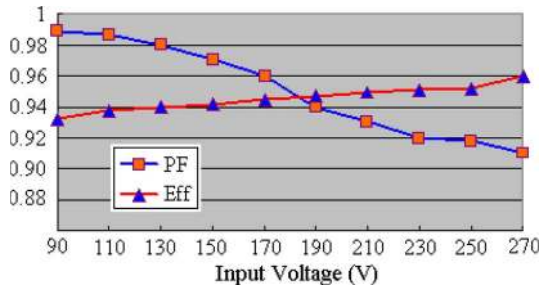
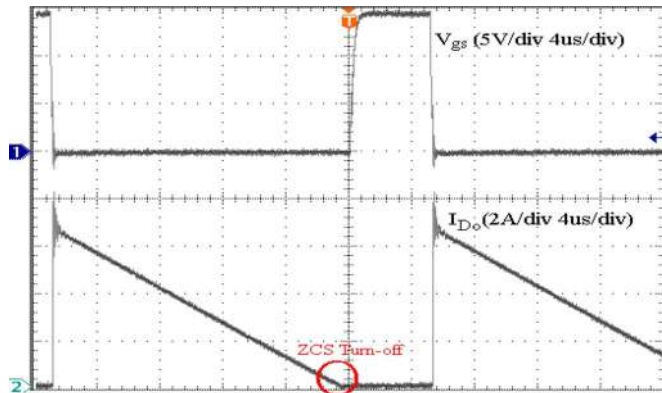Fig. 13. Measured efficiency and power factor variations.

Fig. 14. Output diode current waveform.

In this paper, an improved PWM dimming method is used to control the multiple LED lamp currents. Fig. 15 shows the measured LED lamp currents under different dimming operation conditions. An identify amplitude of 350 mA for four LED lamp currents can be achieved under various dimming operations. The average value of LED lamp currents is regulated by only one PWM controller for adjusting LED lamp brightness. Fig. 16 shows the measured output voltage variations of the LED driver. It can be observed that the LED lamp voltage decreases in accordance with the operating time due to the increased lamp temperature. By using the studied adaptive feedback control, the output voltage of the LED driver can be adjusted to reduce the power losses on the dimming circuit. If the LED strings have different operation junction temperature, the power losses on dimming transistors may be different. In practical design, all LED strings are mounted on a heat sink to have the same temperature condition.

Fig. 17 shows the efficiency variations under different dimming operation conditions. Over 3% efficiency improvement can be obtained at 220-V input under 25% dimming operation by using the studied adaptive feedback control method. The power loss distribution of the studied LED driver under rated load condition is shown in Fig. 18. The power losses caused by a large current ripple on the output winding of the coupled inductor may deteriorate the efficiency performance for a low output voltage design. It can be partially solved by raising the output voltage level. However, an output voltage over 50 V for a LED driver will need an extra isolation design for safety considerations. High voltage stresses on power devices also increase circuit cost and switching losses for a high output voltage design. Anyway, in this paper, we implement a 60-W
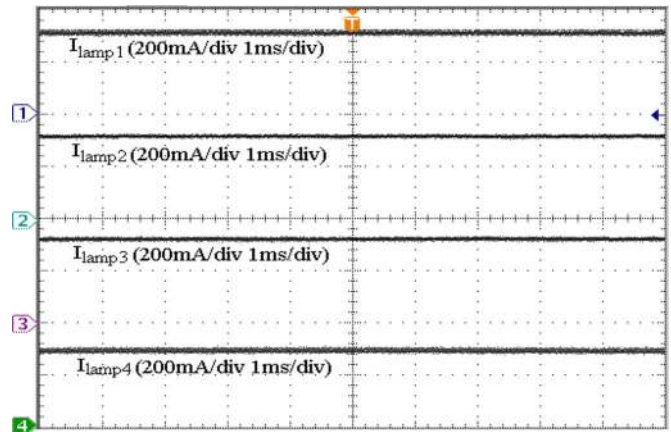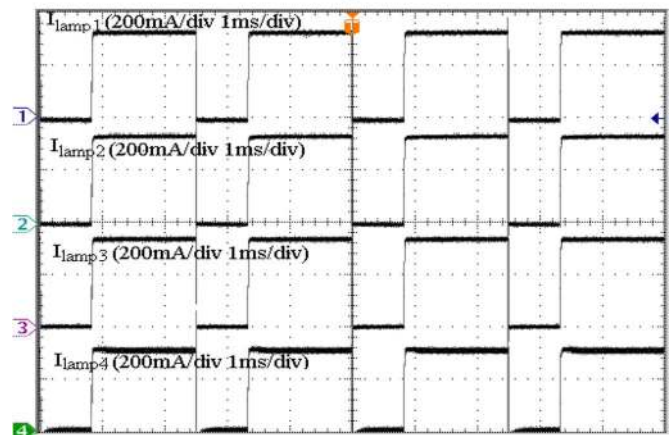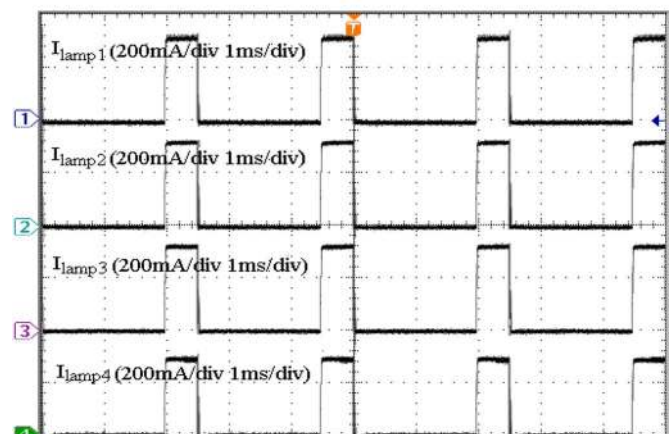
Fig. 15. Measured LED lamp current waveforms under (a) 100%, (b) 70%, and (c) 20% dimming operations.
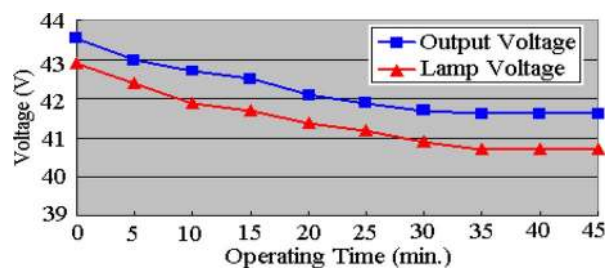

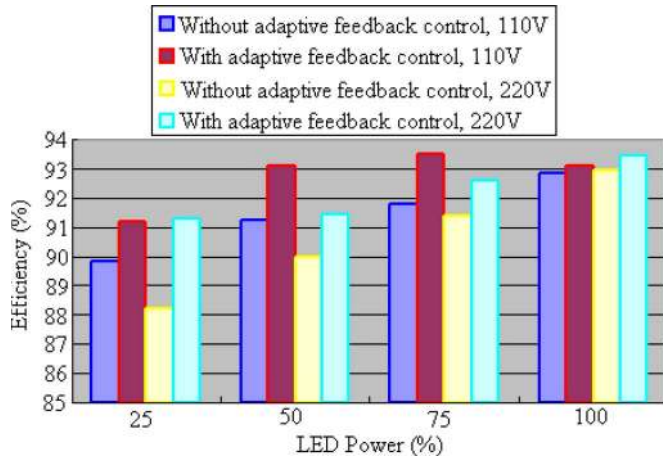Fig. 16. Measured output voltage variations.

Fig. 17. Efficiency comparisons for the LED drivers with and without adaptive feedback control (including dimming circuit).
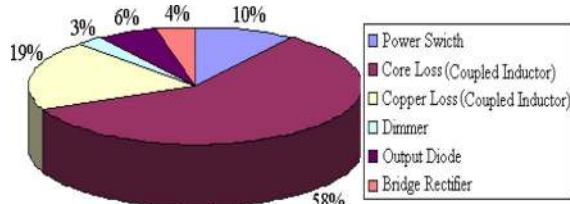

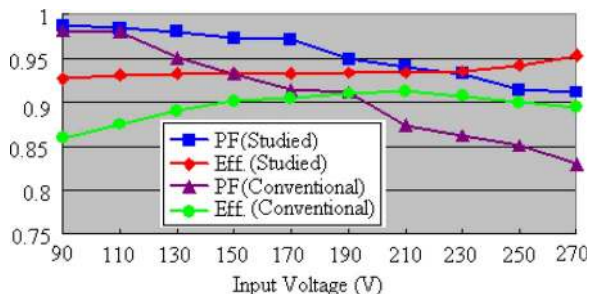Fig. 18. Power loss distribution of the studied LED driver.

Fig. 19. Efficiency comparisons between the studied and conventional LED drivers.

prototype with output voltage around 43 V that presents an excellent efficiency performance by using a simple circuit topology with an adaptive feedback control design. Fig. 19 shows the measured performance comparisons between the studied LED driver with adaptive feedback control and the conventional TM SEPIC PFC topology with constant voltage control. It can be observed that the studied topology has better efficiency and power factor features under universal input voltage operation from 90 to 270 V.

V. CONCLUSION

In this paper, we have presented a dimmable LED driver for low-power lighting applications. Under universal input voltage operation, high efficiency and high power factor can be achieved by a coupled inductor SEPIC PFC converter with an adaptive feedback control design. An improved PWM dimming technique was also studied for regulating the LED current and brightness. Current amplitude of LED lamps can be regulated at a specific condition suggested by the LED's datasheet. A

laboratory prototype was built and tested. The experimental waveforms of the laboratory prototype were shown to verify the feasibility of the proposed scheme.

REFERENCES

[1] C. Y. Wu, T. F. Wu, J. R. Tsai, Y. M. Chen, and C. C. Chen, "Multistring LED backlight driving system for LCD panels with color sequential display and area control," *IEEE Trans. Ind. Electron.*, vol. 55, no. 10, pp. 3791–3800, Oct. 2008.

[2] Maxim-Dallas Semiconductor, Why drive white LEDs with constant current, Jun. 2004.

[3] C. H. Lin, "Digital-dimming controller with current spikes elimination technique for LCD backlight electronic ballast," *IEEE Trans. Ind. Electron.*, vol. 53, no. 6, pp. 1881–1888, Dec. 2006.

[4] S. J. Choi, K. C. Lee, and B. H. Cho, "Design of fluorescent lamp ballast with PFC using a power piezoelectric transformer," *IEEE Trans. Ind. Electron.*, vol. 52, no. 6, pp. 1573–1581, Dec. 2005.

[5] S. K. Kim, H. S. Han, Y. J. Woo, and G. H. Cho, "Detection and regulation of CCFL current and open-lamp voltage while keeping floating condition of the lamp," *IEEE Trans. Ind. Electron.*, vol. 53, no. 2, pp. 707–709, Apr. 2006.

[6] H. J. Chiu, H. M. Huang, H. T. Yang, and S. J. Cheng, "An improved single-stage Flyback PFC converter for high-luminance lighting LED lamps," *Int. J. Circuit Theory Appl.*, vol. 36, no. 2, pp. 205–210, Mar. 2008.

[7] H. J. Chiu and S. J. Cheng, "LED backlight driving system for large-scale of LCD panels," *IEEE Trans. Ind. Electron.*, vol. 54, no. 5, pp. 2751–2760, Oct. 2007.

[8] H. M. Huang, S. H. Twu, S. J. Cheng, and H. J. Chiu, "A single-stage SEPIC PFC converter for multiple lighting LED lamps," in *Proc. 4th IEEE Int. Symp. Electron. Des., Test Appl.*, Jan. 2008, pp. 15–19.

[9] Y. Hu and M. M. Jovanovic, "LED driver with self-adaptive drive voltage," *IEEE Trans. Power Electron.*, vol. 23, no. 6, pp. 3116–3125, Nov. 2008.

[10] G. Moschopoulos and P. Jain, "Single-phase single-stage power-factor-corrected converter topologies," *IEEE Trans. Ind. Electron.*, vol. 52, no. 1, pp. 23–35, Feb. 2005.

[11] C. S. Lin and C. L. Chen, "A novel single-stage push-pull electronic ballast with high input power factor," *IEEE Trans. Ind. Electron.*, vol. 48, no. 4, pp. 770–776, Aug. 2001.

[12] W. Guo and P. K. Jain, "A power-factor-corrected AC-AC inverter topology using a unified controller for high-frequency power distribution architecture," *IEEE Trans. Ind. Electron.*, vol. 51, no. 4, pp. 874–883, Aug. 2004.

[13] F. S. Kang, S. J. Park, and C. U. Kim, "ZVZCS single-stage PFC AC-to-DC half-bridge converter," *IEEE Trans. Ind. Electron.*, vol. 49, no. 1, pp. 206–216, Feb. 2002.

[14] J. J. Lee, J. M. Kwon, E. H. Kim, and B. H. Kwon, "Dual series-resonant active-clamp converter," *IEEE Trans. Ind. Electron.*, vol. 55, no. 2, pp. 699–710, Feb. 2008.

[15] J. A. Villarejo, J. Sebastian, F. Soto, and E. de Jodar, "Optimizing the design of single-stage power-factor correctors," *IEEE Trans. Ind. Electron.*, vol. 54, no. 3, pp. 1472–1482, Jun. 2007.

[16] A. Nasiri, Z. Nie, S. B. Bekiarov, and A. Emadi, "An on-line UPS system with power factor correction and electric isolation using BIFRED converter," *IEEE Trans. Ind. Electron.*, vol. 55, no. 2, pp. 722–730, Feb. 2008.

[17] J. M. Kwon, W. Y. Choi, J. J. Lee, E. H. Kim, and B. H. Kwon, "Continuous-conduction-mode SEPIC converter with low reverse-recovery loss for power factor correction," *Proc. Inst. Elect. Eng.—Electr. Power Appl.*, vol. 153, no. 5, pp. 673–681, Sep. 2006.

[18] H. Macbahi, J. Xu, A. Cheriti, and V. Rajagopalan, "A soft-switched SEPIC based AC-DC converter with unity power factor and sinusoidal input current," in *Proc. 20th Int. Telecommun. Energy Conf.*, Oct. 1998, pp. 663–668.

[19] M. J. Willers, M. G. Egan, S. Daly, and J. M. D. Murphy, "Analysis and design of a practical discontinuous-conduction-mode BIFRED converter," *IEEE Trans. Ind. Electron.*, vol. 46, no. 4, pp. 724–733, Aug. 1999.

[20] X. Wu, X. Xie, Z. Chen, Z. Qian, and R. Zhao, "Low voltage and current stress ZVZCS full bridge DC–DC converter using center tapped rectifier reset," *IEEE Trans. Ind. Electron.*, vol. 55, no. 3, pp. 1470–1477, Mar. 2008.

[21] H. I. Hsieh, J. S. Li, and D. Chen, "Effects of X capacitors on EMI filter effectiveness," *IEEE Trans. Ind. Electron.*, vol. 55, no. 2, pp. 949–955, Feb. 2008.

[22] ST Microelectronics, Application Note AN1056 Design equations of high-power-factor Flyback converters based on the L6561, Sep. 2003.

[23] J. Chen and C. Chang, "Analysis and design of SEPIC converter in boundary conduction mode for universal–input power factor correction applications," in *Proc. IEEE 32nd Annu. Power Electron. Spec. Conf.*, Jun. 2001, vol. 2, pp. 742–747.

[24] X. Qu, S. C. Wong, and C. K. Tse, "Color control system for RGB LED light sources using junction temperature measurement," in *Proc. 33rd Annu. Conf. IEEE Ind. Electron. Soc.*, Nov. 2007, pp. 1363–1368.

[25] S. Y. R. Hui and Y. X. Qin, "A general photo-electro-thermal theory for light emitting diode (LED) systems," in *Proc. 24th Annu. IEEE Appl. Power Electron. Conf. Expo.*, Feb. 2009, pp. 554–562.

[26] Y. X. Qin, D. Y. Lin, and S. Y. R. Hui, "A simple method for comparative study on the thermal performance of light emitting diodes (LED) and fluorescent lamps," in *Proc. 24th Annu. IEEE Appl. Power Electron. Conf.*, Feb. 2009, pp. 152–158.

Huang-Jen Chiu (M'00–SM'09) was born in I-Lan, Taiwan, in 1971. He received the B.E. and Ph.D. degrees in electronic engineering from the National Taiwan University of Science and Technology, Taipei, Taiwan, in 1996 and 2000, respectively.

From August 2000 to July 2002, he was an Assistant Professor with the Department of Electronic Engineering, I-Shou University, Kaohsiung, Taiwan. From August 2002 to July 2006, he was with the Department of Electrical Engineering, Chung-Yuan Christian University, Chung-Li, Taiwan. Since August 2006, he has been with the Department of Electronic Engineering, National Taiwan University of Science and Technology, where he is currently a Professor. His research interests include high-efficiency LED drivers, soft-switching techniques, electromagnetic compatibility issues, power factor correction topologies, electronic ballast, and DSP control in renewable energy applications.

Dr. Chiu is a Senior Member of the IEEE Power Electronics Society. He received the Young Researcher Award from the National Science Council, Taiwan, in 2004.

Yu-Kang Lo (M'96) was born in Chia-Yi, Taiwan, in 1969. He received the B.S. and Ph.D. degrees in electrical engineering from the National Taiwan University, Taipei, Taiwan, in 1991 and 1995, respectively.

Since 1995, he has been with the faculty of the Department of Electronic Engineering, National Taiwan University of Science and Technology, Taipei, where he is currently an Associate Professor and in charge of the Power Electronic Laboratory. His research interests include the design and analysis of a variety of switching-mode power converters and power factor correctors.

Jun-Ting Chen was born in Taichung, Taiwan, in 1969. He received the M.S. degree from the Department of Electronic Engineering, Chung Yuan Christian University, Taoyuan, Taiwan, in 2002. He is currently working toward the Ph.D. degree at the National Taiwan University of Science and Technology, Taipei, Taiwan.

His research interests include the design and analysis of a variety of switch-mode power converters and electronic circuit design.

Shih-Jen Cheng was born in Kinmen, Taiwan, in 1981. He received the B.E. degree in electrical engineering from Kao-Yuan University, Kaohsiung, Taiwan, in 2005 and the M.S. degree in electrical engineering from Chung-Yuan Christian University, Chung-Li, Taiwan, in 2007. He is currently working toward the Ph.D. degree at the National Taiwan University of Science and Technology, Taipei, Taiwan.

His research interests include LED backlight circuit design, field-programmable gate array, and DSP control applications.

Chung-Yi Lin was born in Chia-Yi, Taiwan, in 1984. He received the B.E. degree in electronic engineering from the National Taiwan University of Science and Technology, Taipei, Taiwan, in 2006, where he is currently working toward the Ph.D. degree.

His research interests include the design and analysis of the zero-voltage-switching dc–dc converters, and power factor correction techniques.

Shann-Chyi Mou was born in Taipei, Taiwan, in 1971. He received the Ph.D. degree in power mechanical engineering from the National Tsing Hua University, Hsinchu, Taiwan, in 2004.

Since August 2004, he has been with the Department of Mechanical Engineering, Ching Yun University, Jung-Li, Taiwan. His research interests include linear control theory design of piezoelectric actuator and its application in precision positioning control, copper-indium-gallium-(di) selenide solar cells, asymmetric pulsed-dc plasma sputtering processes, and system identification of biomedical signals for electrocardiogram.